CONFERENCE PRE-PRINT

FDTD SIMULATION OF THE PROPAGATION CHARACTERISTICS OF MILLIMETER-WAVE VORTEX IN MAGNETIZED PLASMA

C. WANG National Institute for Fusion Science Toki, Japan Email: naka-lab@nifs.ac.jp

H. NAKAMURA National Institute for Fusion Science Toki, Japan

H. KAWAGUCHI Muroran Institute of Technology Muroran, Japan

S. KUBO Chubu University Kasugai, Japan

Abstract

Three-dimensional Finite-Difference Time-Domain (FDTD) simulations are employed to investigate the propagation characteristics of millimeter-wave vortex fields in magnetized plasma. A hybrid mode of millimeter-wave vortex is excited in a cylindrical corrugated waveguide and incident to the magnetized plasma. The results show that the hybrid-mode vortex can propagate in high-density plasma regions where conventional plane waves are cut off, and that the penetrated power depends strongly on the topological charge *l*. To further explore the practical implications, the paper also analyzes Laguerre-Gaussian (LG) beams incident from free space to magnetized plasma and then investigates the dependence of topological charge on penetrated power without the waveguide boundaries. These results provide significant potential for developing functional electron cyclotron resonance heating (ECRH) schemes.

1. INTRODUCTION

Optical vortices, characterized by helical wavefronts and the possession of orbital angular momentum (OAM), have attracted considerable attention in diverse scientific fields, ranging from particle manipulation to advanced imaging techniques. Their unique capability of carrying quantized angular momentum makes them a promising candidate for applications in plasma physics [1-7]. In recent years, it has been pointed out that millimeter-wave vortices can propagate in the magnetized plasmas even under conditions where conventional plane waves are cut off [8]. This finding means that ECRH could be extended to high electron density plasmas, where normal plane wave cannot transfer its energy, millimeter-wave vortex can still deliver energy. On the other hand, it is known that hybrid modes excited in corrugated waveguides can carry well-defined OAM and propagate stably [9]. In the previous work, the hybrid mode of millimeter-wave vortex in the cylindrical corrugated waveguide was utilized to investigate millimeter-wave vortex plasma heating [10-11].

In realistic experiments, hybrid modes in waveguides should be transformed into LG beams in free space, for example by using a spiral phase mirror (SPM), before being incident into plasma. Preliminary attempts at plasma heating with optical vortices have been carried out in devices such as LHD and Heliotron-J. However, insufficient topological charge or low conversion efficiency in the conversion to LG beams. On the other hand, a new basic experiment is being planned, including fundamental studies of microwave vortex propagation in the HYPER-I device. These developments motivate a systematic theoretical and numerical investigation of vortex propagation in magnetized plasma. In particular, it is essential to clarify how the penetrated power depends on the topological charge, and to investigate the behavior of free-space LG-modes. The paper demonstrates the propagation characteristics of millimeter-wave LG-modes by using FDTD simulations, focusing on their ability to penetrate high electron density plasma regions.

2. NUMERICAL MODEL AND METHODOLOGY

2.1 Millimeter-wave vortex of LG-mode in free space



FIG.1 Laguerre-Gaussian beam

The propagation of LG-mode millimeter-wave vortex in magnetized plasma was analyzed using a full 3D FDTD simulation. And the LG-mode is a well-known solution to the paraxial approximation of the Helmholtz equation in cylindrical coordinates, expressed as (*FIG.1*),

in cylindrical coordinates, expressed as
$$(FIG.I)$$
,
$$E(r,\emptyset,z) = \frac{c}{\left(1 + \frac{z^2}{z_R^2}\right)^{\frac{1}{2}}} \left(\frac{\sqrt{2}r}{w(z)}\right)^l L_p^l \left(\frac{2r^2}{w^2(z)}\right) \exp\left(\frac{-r^2}{w^2(z)}\right) \exp\left(\frac{-ikr^2z}{2(z^2 + z_R^2)}\right) \exp\left(\frac{i(2p + l + 1)\tan^{-1}\frac{z}{z_R}\right), \tag{1}$$

where L_p^l is Laguerre polynomial, w(z) is beam radius, z_R is Rayleigh range. The azimuthal indel l corresponds to the topological charge of the vortex beam, while the radial index p determines the number of the radial nodes. In the simulations, the LG field profile was implemented as the initial condition at the entrance plane of the computational domain. The input frequency was set to 84 GHz with a total power of 1MW, and the polarization was along the x-axis. If we define Poynting power P on the surface S of the LG-mode as follows,

$$P = \frac{1}{2T} \int_0^T dt \int_S (\mathbf{E} \times \mathbf{H}^*) \cdot d\mathbf{S}, \tag{2}$$

where *T* is the time period. We here consider that the LG-mode millimeter-wave vortex, which is illuminated to the magnetized plasma (see *FIG.2*) from free space. Examples of distributions of electric field intensity of LG-mode vortex fields in *x-y* vertical cross section are depicted in *FIG.2*.

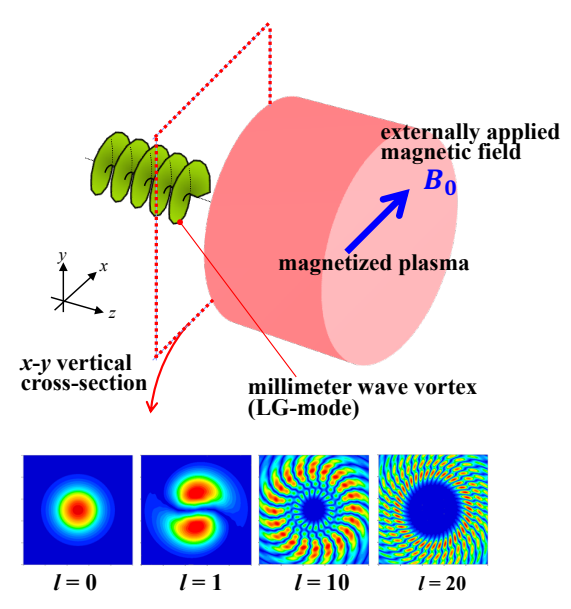


FIG.2 Configuration of plasma heating by LG-mode

2.2 Macro-model of magnetized plasma

Since a full coupling analysis between electromagnetic waves and plasma particles requires extremely large computational cost, a macroscopic model was adopted for describing the plasma response. In this study, the Drude-Lorentz dispersive model was employed to represent the behavior of magnetized plasma. The electron displacement density vector P and the current density vector J = dP/dt were used as the fundamental plasma variables. Their evolution is governed by the following equation:

$$\frac{d\mathbf{J}}{dt} + \gamma \mathbf{J} + \omega_0^2 \mathbf{P} = \varepsilon_0 \omega_p^2 \left(\mathbf{E} + \frac{1}{n_e q_e} \mathbf{J} \times \mathbf{B}_0 \right), \tag{3}$$

where γ is the damping coefficient, n_e is the electron density, q_e is the elementary charge, and \boldsymbol{B}_0 is the externally applied magnetic field. $\omega_p = \sqrt{q_e^2 n_e/\varepsilon_0 m_e}$ is a plasma angular frequency. This formulation allows the plasma to be represented as a dispersive medium with frequency-dependent response, while keeping manageable computational cost within FDTD schemes.

2.3 FDTD formulation for millimeter-wave vortex propagation in magnetized plasma

The FDTD analysis of the propagation of millimeter-wave vortex in magnetized plasma was performed by coupling discretized Maxwell's equations on a 3D grid with the macroscopic plasma model. The electric and magnetic field components E and H were updated as follows,

$$\boldsymbol{E}^{n+1} = \frac{\frac{\varepsilon_0}{\Delta t} - \frac{\sigma}{2}}{\frac{\varepsilon_0}{\Delta t} + \frac{\sigma}{2}} \boldsymbol{E}^n + \frac{1}{\frac{\varepsilon_0}{\Delta t} + \frac{\sigma}{2}} \nabla \times \boldsymbol{H}^{n+\frac{1}{2}} - \frac{1}{\frac{\varepsilon_0}{\Delta t} + \frac{\sigma}{2}} \boldsymbol{J}^{n+\frac{1}{2}},$$

$$\boldsymbol{H}^{n+\frac{1}{2}} = \boldsymbol{H}^{n-\frac{1}{2}} - \frac{\Delta t}{\mu_0} \nabla \times \boldsymbol{E}^n,$$

$$(4-1)$$

$$H^{n+\frac{1}{2}} = H^{n-\frac{1}{2}} - \frac{\Delta t}{\mu_0} \nabla \times E^n, \tag{4-2}$$

and the magnetized plasma macro-model (3) for P and J,

$$\mathbf{P}^{n+1} = \Delta t \mathbf{J}^{n+\frac{1}{2}} + \mathbf{P}^n, \tag{5-1}$$

$$\mathbf{P}^{n+1} = \Delta t \mathbf{J}^{n+\frac{1}{2}} + \mathbf{P}^{n}, \qquad (5-1)$$

$$\frac{\mathbf{J}^{n+\frac{1}{2}} - \mathbf{J}^{n-\frac{1}{2}}}{\Delta t} + \gamma \frac{\mathbf{J}^{n+\frac{1}{2}} + \mathbf{J}^{n-\frac{1}{2}}}{2} + \omega_0^2 \mathbf{P}^n = \varepsilon_0 \omega_p^2 \mathbf{E}^n + \frac{\varepsilon_0 \omega_p^2}{q_e n_e} \frac{\mathbf{J}^{n+\frac{1}{2}} + \mathbf{J}^{n-\frac{1}{2}}}{2} \times \mathbf{B}_0, \qquad (5-2)$$

where ε_0 and μ_0 are the permittivity and permeability of free space, and σ is the conductivity. Δt is the temporal step size, E and P are assigned to integer time steps, H and J are assigned to half integer time steps, that is, E and P or H and J are calculated simultaneously. In particular, it is necessary to solve the following matrix equation for (5-2) to obtain each component of J in every time-step,

equation for (5-2) to obtain each component of
$$J$$
 in every time-step,
$$\begin{pmatrix}
\frac{1}{\Delta t} + \frac{\gamma}{2} & -\frac{\varepsilon_0 \omega_p^2}{q_e n_e} \frac{B_{z0}}{2} & \frac{\varepsilon_0 \omega_p^2}{q_e n_e} \frac{B_{y0}}{2} \\
\frac{\varepsilon_0 \omega_p^2}{q_e n_e} \frac{B_{y0}}{2} & \frac{1}{\Delta t} + \frac{\gamma}{2} & -\frac{\varepsilon_0 \omega_p^2}{q_e n_e} \frac{B_{z0}}{2} \\
-\frac{\varepsilon_0 \omega_p^2}{q_e n_e} \frac{B_{z0}}{2} & \frac{\varepsilon_0 \omega_p^2}{q_e n_e} \frac{B_{y0}}{2} & \frac{1}{\Delta t} + \frac{\gamma}{2}
\end{pmatrix}
\begin{pmatrix}
\int_{x}^{n+\frac{1}{2}} \\
J_{x}^{n+\frac{1}{2}} \\
J_{x}^{n+\frac{1}{2}}
\end{pmatrix} = \begin{pmatrix}
(-\frac{1}{\Delta t} + \frac{\gamma}{2})J_{x}^{n-\frac{1}{2}} + \frac{\varepsilon_0 \omega_p^2}{2q_e n_e} (J_{y}^{n-\frac{1}{2}}B_{z0} - J_{z}^{n-\frac{1}{2}}B_{y0}) + \varepsilon_0 \omega_p^2 E_{x}^{n} - \omega_0^2 P_{x}^{n} \\
(-\frac{1}{\Delta t} + \frac{\gamma}{2})J_{y}^{n-\frac{1}{2}} + \frac{\varepsilon_0 \omega_p^2}{2q_e n_e} (J_{z}^{n-\frac{1}{2}}B_{x0} - J_{x}^{n-\frac{1}{2}}B_{z0}) + \varepsilon_0 \omega_p^2 E_{y}^{n} - \omega_0^2 P_{y}^{n} \\
(-\frac{1}{\Delta t} + \frac{\gamma}{2})J_{z}^{n-\frac{1}{2}} + \frac{\varepsilon_0 \omega_p^2}{2q_e n_e} (J_{x}^{n-\frac{1}{2}}B_{y0} - J_{y}^{n-\frac{1}{2}}B_{x0}) + \varepsilon_0 \omega_p^2 E_{z}^{n} - \omega_0^2 P_{z}^{n}
\end{pmatrix}, \tag{6}$$

3. NUMERICAL EXAMPLES

The numerical model for simulating the propagation of millimeter-wave vortex fields in magnetized plasma is depicted in FIG.3. A LG-mode millimeter-wave vortex with topological charge l was introduced at a distance of two wavelengths from the perfectly matched layer (PML). The LG-mode beam then propagated through the vacuum region before entering the magnetized plasma. The computational domain was discretized into 600 × 600 × 600 cells with a uniform grid spacing of 0.15 mm. The frequency and input power of the incident vortex were set to 84 GHz and 1MW, respectively. The plasma density and external magnetic field were taken as

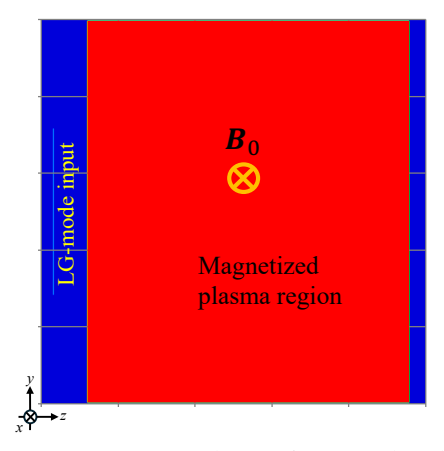


FIG.3 FDTD simulation of numerical model

 $n_e = 1.1 \times 10^{20} \ m^{-3}$ and $|B_0| = 2 \text{T}$, respectively, with the magnetic field oriented along the x-axis. The incident vortex field was linearly polarized in the x-direction.

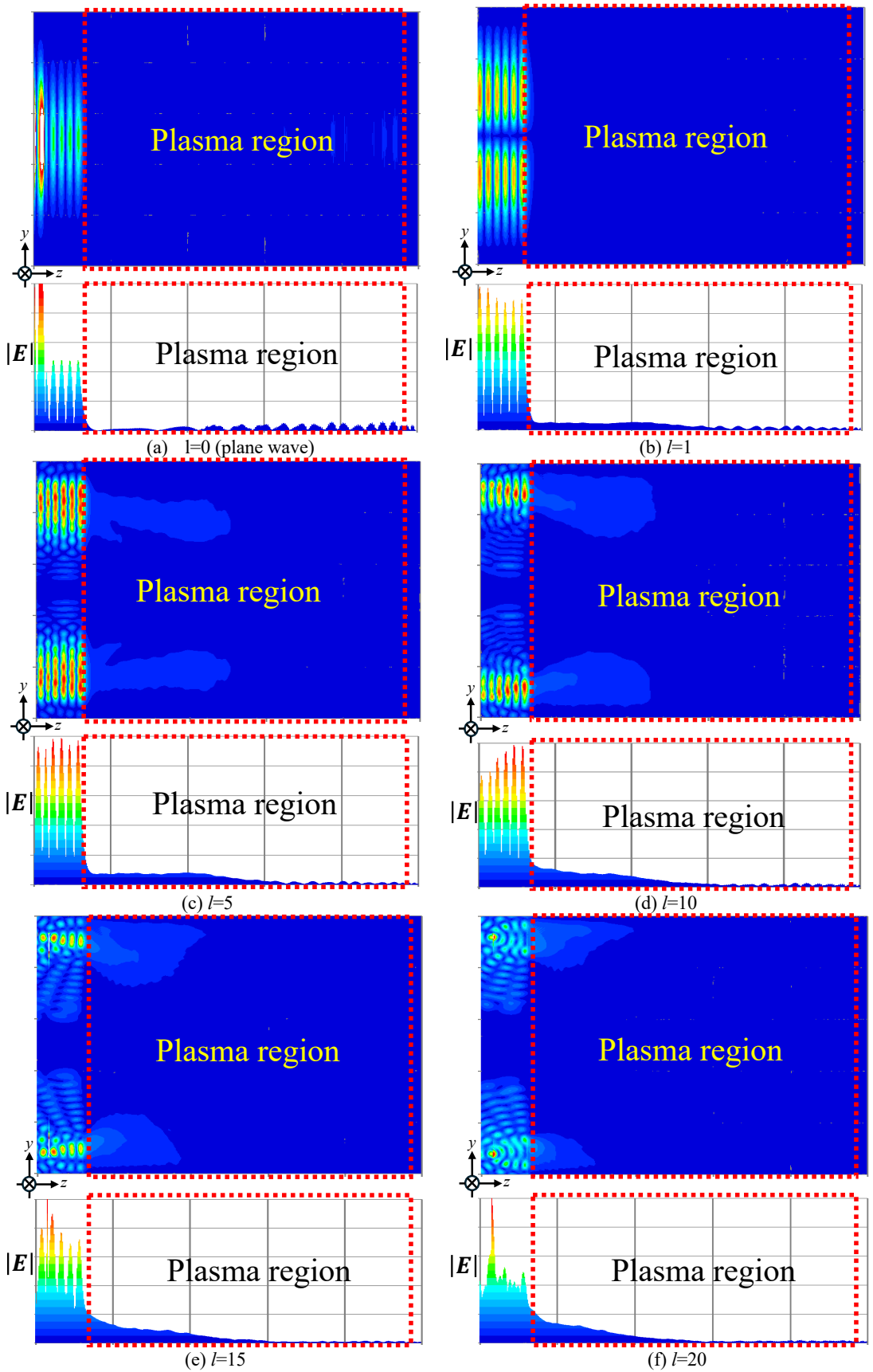


Fig.4 Electric field intensity in y-z plane

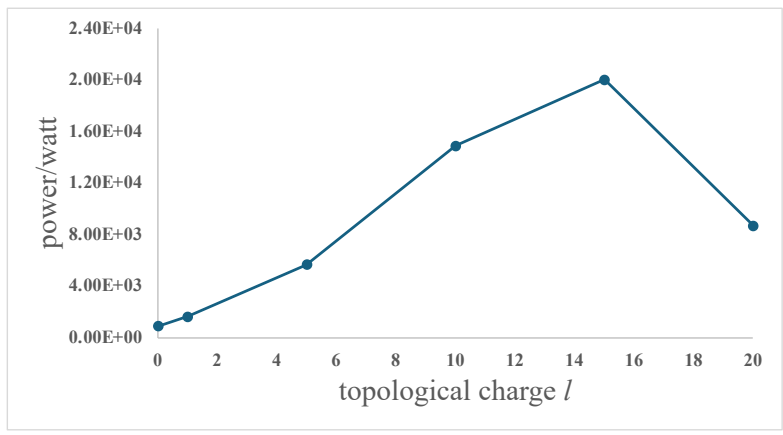


FIG.5 Penetrated power of LG-mode in the magnetized plasma

FIG.4 shows the distributions of the electric field intensity in the y-z plane for different values of the topological charge: (a) l=1 (plane wave), (b) l=1, (c) l=5, (d) l=10, (e) l=15, and (f) l=20. The results clearly confirm that the LG-mode millimeter-wave vortex can propagate into the magnetized plasma region, even under conditions where the normal plane wave (l=0) is cut off. This indicates that similar phenomena observed for hybrid-mode vortices can also be realized in the LG-mode vortex case.

The dependence of the penetrated power on the topological charge l is plotted in FIG.5. It can be seen from the simulation results that the penetrated power of millimeter-wave vortex in the magnetized plasma is strongly dependent on the topological charge l, with a maximum around l=15. This peak behavior is observed even though the waveguide effect is absent in the LG-mode excitation. Indeed, the LG-mode propagates in free space, as the increase of the topological charge l, the higher-order LG-mode beams generally exhibit stronger divergence, with the divergence rate increasing proportionally with the topological charge l and radial index p of the beam. This increased divergence is due to the expanded transverse size of LG-modes, which leads to greater beam spreading as they propagate. This divergence ultimately limits the coupling efficiency into plasma.

4. CONCLUSIONS

Three-dimensional FDTD simulations were carried out to investigate the propagation characteristics of millimeter-wave vortex beams in magnetized plasma. A LG-mode was introduced from free space into the plasma, and its penetration properties were analyzed for different topological charges. The results confirm that LG-mode vortices can propagate in plasma regions where conventional plane waves are cut off condition. The simulations show that the penetrated power strongly depends on the topological charge. While the penetrated power increases with *l* at low and intermediate orders, a maximum is observed around *l*=15, followed by a decrease for higher-order vortices. This reduction is attributed to the enhanced divergence and scattering of high-order LG beams, which limits their coupling efficiency into the plasma. These findings indicate that both the mode structure and the choice of topological charge are critical parameters for optimizing vortex-based plasma heating schemes. The present study highlights the feasibility of employing millimeter-wave vortices for functional plasma heating and provides theoretical guidance for ongoing and future experimental efforts, such as those planned in the HYPER-I device. In the next stage of research, simulations will be extended to plasmas with non-uniform electron density, in order to clarify the influence of realistic density distribution on vortex propagation and energy deposition. These findings provide theoretical guidance for optimizing ECRH schemes, and future work will extend the simulations to more realistic plasma profiles and experimental configurations.

ACKNOWLEDGEMENTS

The computation was performed using Research Center for Computational Science, Okazaki, Japan (Project: 25-IMS-C100) and Plasma Simulator of NIFS. The research was supported by KAKENHI (Nos. 21H04456, 22K03572, 23K03362, 23K11190, 24K00613, 25H01640), by the NINS program of Promoting Research by Networking among Institutions (01422301) by the NIFS Collaborative Research Programs (NIFS24KIG002, NIFS25KIST062, NIFS25KIIT019).

REFERENCES

- [1] ALLEN, L., et al., Orbital angular momentum of light and the transformation of Laguerre-Gaussian laser modes. Phys. Rev. A 45 (1992) 8185.
- [2] BABIKER, M., et al., Orbital angular momentum exchange in the interaction of twisted light with molecules, Phys. Rev. Lett. 89 (2002) 143601.
- [3] ANDERSEN, M. F., et al., Quantized rotation of atoms from photons with orbital angular momentum, Phys. Rev. Lett. 97 (2006) 170406.
- [4] VAN VEENENDAAL, M., MCNULTY, I., Prediction of strong dichroism induced by x rays carrying orbital momentum. Phys. Rev. Lett. 98 (2007) 157401.
- [5] MATSUBA, S., et al., Generation of vector beam with tandem helical undulators, Appl. Phys. Lett. 113 (2018), 021106.
- [6] KAWAGUCHI, H., KATOH, M., Orbital angular momentum of Liénard–Wiechert fields. Progress of Theoretical and Experimental Physics, 8(2019), 083A02.
- [7] KAWAGUCHI, H., NAKAMURA, H., Evaluation of mechanical torque acting on scatterer in microwave vortex fields, IEEE Microw. Wireless Compon. Lett. 29 (2019) 504-506.
- [8] TSUJIMURA, T, I., KUBO. S., Propagation properties of electron cyclotron waves with helical wavefronts in magnetized plasma, Phys. Plasmas 28 (2021) 012502.
- [9] KAWAGUCHI, H., KUBO, S., NAKAMURA, H., Orbital angular momentum of vortex fields in corrugated cylindrical waveguide hybrid mode, IEEE Microw. Wireless Technol. Lett. 33 (2022) 118-121.
- [10] WANG, C., KAWAGUCHI, H., NAKAMURA, H., KUBO, S., The study of propagation characteristics of the millimeter-wave vortex in magnetized plasma by using the FDTD method, Jpn. J. Appl. Phys. 63 (2024) 09SP08.
- [11] WANG, C., KAWAGUCHI, H., NAKAMURA, H., KUBO, S., Consideration on relation between penetrated power and topological charge of millimeter-wave vortex in magnetized plasma, J. Adv. Simul. Sci. Eng. 12 (2025) 145-151.

BIBLIOGRAPHY

SWANSON, D. G., Plasma Waves, 2nd Edition., Institute of Physics Publishing, Bristol and Philadelphia (2003).